Laser and Particle Beams (2016), *34*, 663–668.

doi:10.1017/S0263034616000628

Incident ion charge state dependence of the visible light emission of Xe^{q+} ions bombarding aluminum

Y. GUO,[1,2] Z. YANG,[1] Q. XU,[1,2] J. REN,[3] H. ZHAO,[1] AND Y. ZHAO[3]

[1]Institute of Modern Physics, Chinese Academy of Sciences, Lanzhou, 730000, People's Republic of China
[2]Institute of Modern Physics, University of Chinese Academy of Sciences, Beijing, 100049, People's Republic of China
[3]Department of Applied Physics, Xi'an Jiaotong University, Xi'an, 710049, People's Republic of China

(Received 14 July 2016; Accepted 5 September 2016)

Abstract

In this work, we studied the photon emission in the visible light range for Xe^{q+} ions of different charge states ($10 \le q \le 21$) bombardment on an aluminum target at 410 keV. During the interactions, the spectra in wavelength range 300–500 nm are recorded, including the photons from Al atoms and neutralized Xe^{+} ions. The yield of the visible light strongly depends on the projectile charge states. Its variation tendency with the charge states is similar to that of the potential energy variation. In addition, the experimental results also indicate that when the incident charge state is less than the critical charge state, it obeys the staircase classical-over-barrier model.

Keywords: Highly charged ion; Neutralization; Potential energy; Visible light

1. INTRODUCTION

When a highly charged ion (HCI) bombards a target surface, the potential energy stored in it will be liberated within a rather short time (fs) on a very small surface area (nm). The release of energy will lead to not only the emission of electrons and photons, but surface modification and target sputtering. Specifically, when a HCI interacts with the metal surface, it becomes neutralized by resonant electron transfer from the target surface to highly excited states of the HCI. De-excitation of these states cause the Auger electron and photon emission through the electrons quick cascade transition to the empty shells. Theoretical picture for the neutralization mechanisms and the energy releasing process of the highly charged ions approaching the metal surface has been given within the framework of the classical-over-barrier (COB) model (Burgdörfer *et al.*, 1991). During the neutralization process of the HCI, the target atoms will be excited, ionized or sputtered, simultaneously. The physical picture for this model has been widely used in numerous reports (Lemell *et al.*, 1996; Hägg *et al.*, 1997; Ducrée *et al.*, 1998; Zhang *et al.*, 2011; Song *et al.*, 2015).

Slow HCIs, when compared with single charged ions, is that they carry a large amount of potential energy, which is the sum total of the ionization energies of the removed electrons. Many potential applications of the HCIs have been realized for the recent decays. For example, I. C. Gebeshuber *et al.* using 500 eV Ar^{+} and Ar^{7+} ions bombarding Al_20_3 (0001) single crystal surface found that the observed defect size (both height and lateral dimension) increases with projectile charge state. In terms of the feature, HCIs can be used as a tool for surface modification. Meanwhile, the strong coulomb field carried by HCIs will lead to atomic polarization and capture abundant electrons far away from the solid surface so that the absorbed C, H, and O atoms are removed. Hence, slow HCIs also used as surface cleaning tools.

On the other hand, slow HCIs interaction with the solid also provides information such as electron configuration, multi-interaction, ionization, excitation and charge transfer for the basic research (Ryufuku *et al.*, 1980; Niehaus, 1986; Sekioka *et al.*, 1998; Winter & Aumayr, 2002; Hoffmann *et al.*, 2005; Bajales *et al.*, 2008; Wang *et al.*, 2009). What is more, the understanding on the heavy HIC structure and relevant collision processes has a special meaning for inertial confinement fusion (ICF) research because both the energy losses and the photon emission from X-ray to visible light by heavy HICs could be used to study target implosion dynamics, the coupling of beam-target material and the equation of state (EOS) of thermal plasma physics (Dietrich *et al.*, 1990; Golubev *et al.*, 2001; Walmsley *et al.*, 2001; Hoffmann *et al.*, 2007; Zhao *et al.*, 2012).

Address correspondence and reprint requests to: Z. Yang, Institute of Modern Physics, Chinese Academy of Sciences, Lanzhou, 730000, People's Republic of China. E-mail: z.yang@impcas.ac.cn

Up to now, many experiments or theories in ion-solid collisions focus on the investigation of secondary electrons, sputtering ion or characteristic X-rays emission by the slow projectile (Sporn *et al.*, 1997; Schenkel *et al.*, 1999; Kudo *et al.*, 2000; Zhao *et al.*, 2005; Mei *et al.*, 2012; Xu *et al.*, 2012; Zeng *et al.*, 2012; Ren *et al.*, 2015). However, very few studies involve the visible light emission and its charge state dependence measurements; especially scare studies focus on the quantitative dependence of the visible light emission intensity on the charge state in theory field (Rajasekar *et al.*, 2006; Jadoual *et al.*, 2014; Sakurai *et al.*, 2016). Hence, our present work concentrates on the visible light emission during the slow highly charged Xe^{q+} ions with different charge states ($10 \le q \le 21$) bombardment on the Al surface. In this paper, we primarily exhibit results of light emission from both neutralized Xe^{+} ions and Al atom at the wavelength range 300–500 nm. Besides, the intensities of the photon emission have a strong dependence on the incident charge states, which is similar to the variation of the potential energy versus the q. It indicates that our results agree well with the staircase COB model (Ducrée *et al.*, 1998).

2. EXPERIMENTAL SET-UP

The experiment was carried out at the 320 kV high-voltage platform at the Institute of Modern Physics, Chinese Academy of Sciences, using a high-charge state all permanent Electron Cyclotron Resonance Ion Source. It was designed to be operated at 14.5 GHz with the purpose of producing medium charge state and high charge state gaseous and also metallic ion beams (Sun *et al.*, 2007). The highly charged Xe^{q+} ions provided by it, and then are injected into our target chamber. A schematic drawing of the experiment set-up is shown in Figure 1. Specifically, Xe^{q+} ion beams of 410 keV were collimated to a diameter 5 mm first, and were directed onto a pure aluminum (99.99%) surface at 45° angle with respect to surface normal direction. The thickness of the target is 50 μm. The emitted photons were collected by a quartz lens system, and were focused into entrance silt (A) of the Sp-2558 spectrometer. The spectrometer is equipped with a 1200 G/mm grating blazed at 500 nm and a R955 photomultiplier (PMT) tube, which receives the photon single from the exit slit (B) of the spectrometer. The spectra were collected

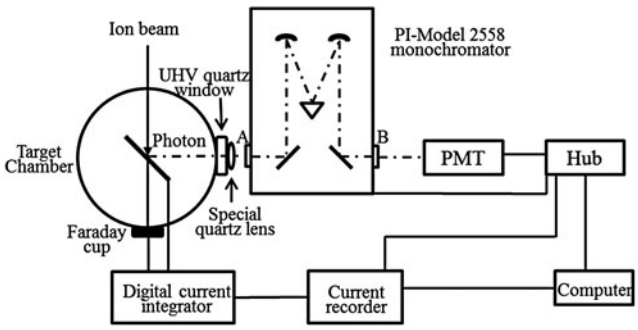

Fig. 1. A schematic drawing of the experiment set-up.

using a step size of 0.02 nm and an integration time of 1000 ms. The detailed route of the photon is shown in the set-up figure as the dotted lines. In order to reduce the background noise, the PMT tube was cooled to −20°C used a semiconductor refrigeration device during the experiment. The PMT tube output and high-voltage power were controlled with a data acquisition system Spectra Hub. The PMT tube output signal in Spectra Hub was amplified, digitized, and recorded by a computer. During experimental measurement, in order to collect as much photons as possible and ensure a better spectral resolution, the entrance silt was 200 μm. And, the beam intensity was about 138 nA. The basic pressure of target chamber was 2×10^{-8} mbar. A mercury lamp was used for wavelength calibration.

In order to eliminate the influence of the ion current fluctuation and the secondary electron emission of the target surface during spectral measurement, we developed a current recorder controlled by a computer. The recorder can monitor the incident ion number and target current at each data point in real time for normalized spectral data. Using it, the spectral normalization method is given by $Y_\lambda = N_\lambda/(I_t/c \times e \times q)$ $(C = (\bar{I}_{ta}/\bar{I}_{fa}))$, where $\bar{I}_{ta}$ and $\bar{I}_{fa}$ are the average current value of incident ion on target and on the Faraday cup, which is obtained by the current recorder in the same condition before the experiment, respectively, hence, the secondary electron emission is excluded; Y_λ (arb. unit) is the normalized photon yield according to each step; N_λ is the photon counts recorded by the computer in each step; I_t is current of incident ion on the target, which also corresponds to each wavelength (λ) point during the measurement; q is charge state of the incident ions, and $e = 1.6 \times 10^{-19}$ C.

3. RESULTS AND DISCUSSION

Figure 2 shows typical normalized spectra from 410 keV Xe^{q+} ions collision with the Al surface. Spectra are recorded in the 300–500 nm wavelength range with 200 μm entrance silt and a spectral resolution of 0.1 nm. A comparison of

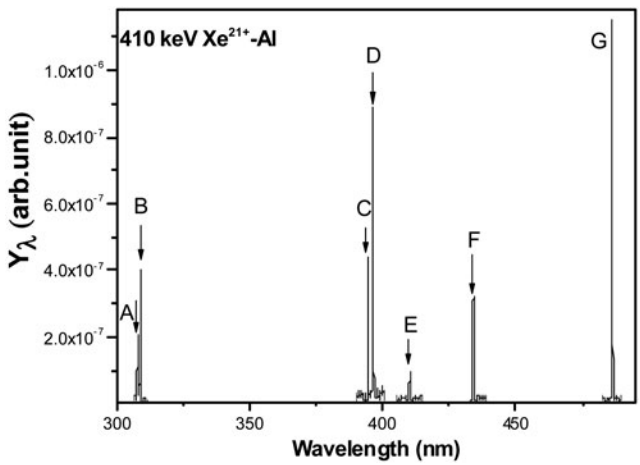

Fig. 2. Normalized optical emission spectrum during 410 keV Xe^{21+} in the visible light range.

https://doi.org/10.1017/S0263034616000628 Published online by Cambridge University Press

Table 1. *Observed lines in the 300–500 nm wavelength range in the Xe^{q+}-Al at 410 keV collision energies. The measured spectral resolution is 0.1 nm and the wavelength unit is nm*

Peak	Origin	Observed wavelength	NIST wavelength	Transition configuration	(Δn, Δl)
A	Al I	308.10	308.2153	$3s^23d(^2D_{3/2})$-$3s^23p(^2P^0_{1/2})$	(0, 1)
B	Al I	309.19	309.284/309.271	$3s^23d(^2D_{3/2,5/2})$-$3s^23p(^2P^0_{3/2})$	(0, 1)
C	Al I	394.52	394.401	$3s^24$ s $(^2S_{1/2})$-$3s^23p$ $(^2P^0_{1/2})$	(1, −1)
D	Al I	396.28	396.152	$3s^24$ s $(^2S_{1/2})$-$3s^23p$ $(^2P^0_{3/2})$	(1, −1)
E	Xe II	410.22	410.310	$5p^4(^1D_2)6d\ ^2[2]_{5/2}$-$5p^4(^1D_2)6p\ ^2[1]^\circ_{3/2}$	(0, 1)
F	Xe II	434.12	434.256	$5p^4(^3P_2)8$ s $^2[2]_{5/2}$-$5p4(^3P_1)6p\ ^2[1]^\circ_{3/2}$	(2, −1)
G	Xe II	486.11	486.245	$5p^4(^3P_2)7$ s $^2[2]_{5/2}$-$5p^4(^3P_2)6p\ ^2[2]^\circ_{5/2}$	(1, −1)

these spectra with the NIST data (Eriksson & Isberg, 1963) indicates that they contain spectral lines resulting from the radiative de-excitation of excited target atoms and neutralized projectile ions. Specifically, the spectral lines A–E correspond to transition configuration and other formations are listed in the following table. From the table, one can see that the experimental results agree well with the data given by the NIST.

According to the COB model, during collisions, when the distance between HCIs and the metal surface reaches a critical distance $R_C \sim \sqrt{2q}/W$, one or multiple electron can be resonantly captured from the metal surface into projectile highly excited states $n_c \sim q/\sqrt{2W}$, where, q is the incident charge state and W is the work function of the metal surface (atomic units are used). This resonant charge transfer process lasts until the ion is almost fully neutralized and a hollow atom/ion is formed, which is called the first generation hollow atom/ion (HA1). The time T for the HA1 arriving at the above surface is about R_C/v (SI units are used). In the present experiment, W(Al) is 0.154 a.u, v is 7.74×10^5 m/s, therefore, for $q = 10$, $R_C \sim 29.04$ a.u, $n_c \sim 18$, $T = 1.97 \times 10^{-15}$ s, and for $q = 21$, $R_C \sim 42.08$ a.u, $n_c \sim 38$, $T = 2.88 \times 10^{-15}$ s, respectively. That is, in our experiment, the time for HA1 arriving at the above surface is about 10^{-15} s. As we know, the time for HA1 to exist is about 10^{-14}–10^{-13} s, which is larger than T. It indicates that HA1 is no decay when it reaches the above surface. So, at the time HA1 impact onto the metal surface, the electrons in the high states are stripped off. Subsequently, the ions enter into the below surface and a new hollow atom/ion (HA2) is formed and the electrons filled into much lower shells than HA1. Table 1 tells us that, in our experiment, the electrons filled into $n = 6$, 7, 8 of the HA2. On the other hand, during the projectile neutralization process mentioned above, the potential energy of the highly charged Xe^{q+} ions is released in the metal surface and excites the target atoms. In the present work, Al 3p electrons is excited to 3*d* or 4 s shell as shown in Table 1. The excited atoms de-excite and the Al I visible lights emit.

In addition, we also observed that the photon yields, including the Al I and Xe II spectra, obviously increase with the increasing charge states. The normalized spectra A, B, C, D, E, F, and G induced by Xe^{q+} ions with the different charge states are shown in Figures 3–7.

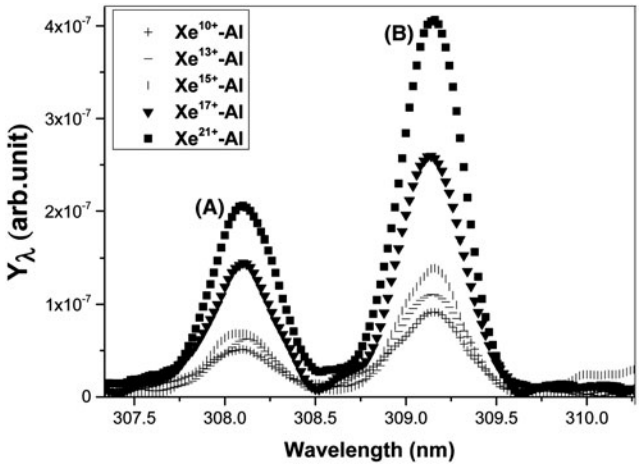

Fig. 3. Normalized spectra at 308.10 (A) and 309.19 nm (B) by different incident charge states.

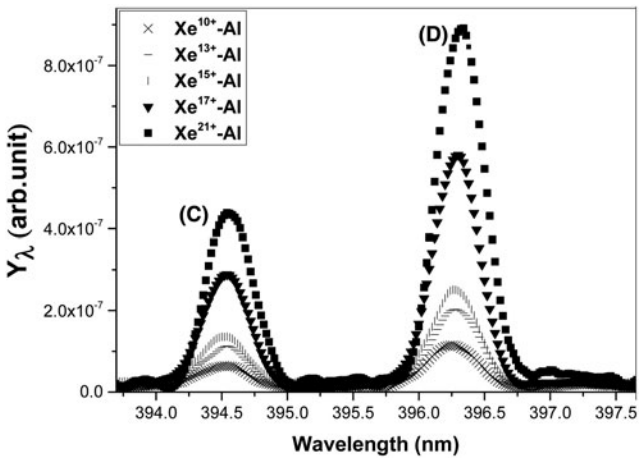

Fig. 4. Normalized spectra at 394.52 (C) and 396.28 nm (D) by different incident charge states.

Obviously, as can be seen from the figures, the photon yields are increasing with the q for the same incident energy. It indicates that the yields of the visible light emissions basically depend on how much potential energy of the incident ions is transferred and deposited on the surface atoms. More clearly, both the intensities of the Al I spectra

https://doi.org/10.1017/S0263034616000628 Published online by Cambridge University Press

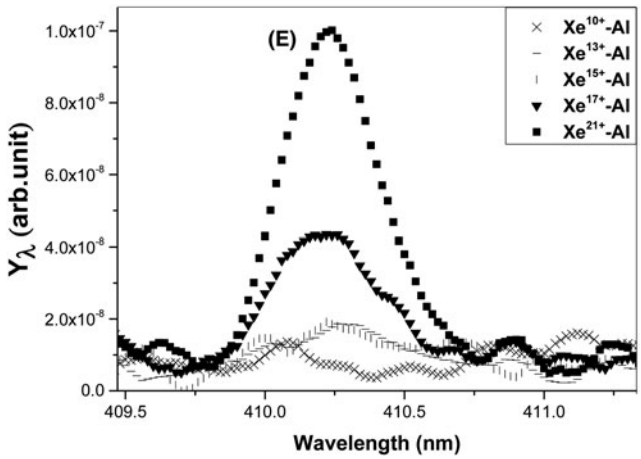

Fig. 5. Normalized spectrum at 410.22 nm (E) by different incident charge states.

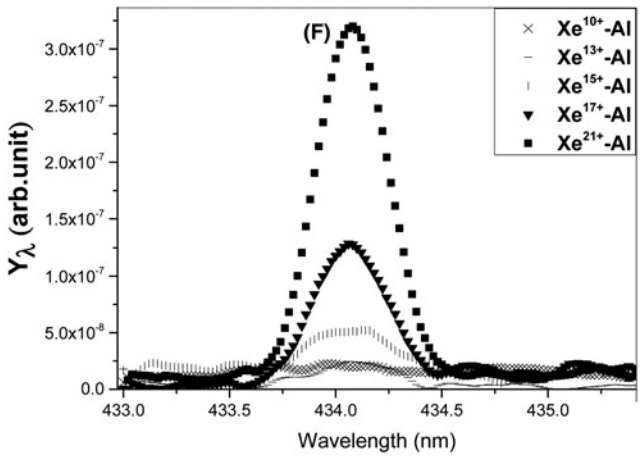

Fig. 6. Normalized spectrum at 434.12 nm (F) by different incident charge states.

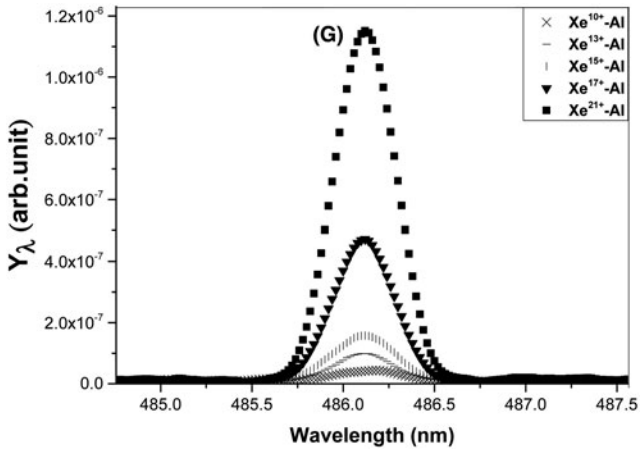

Fig. 7. Normalized spectrum at 486.11 nm (G) by different incident charge states.

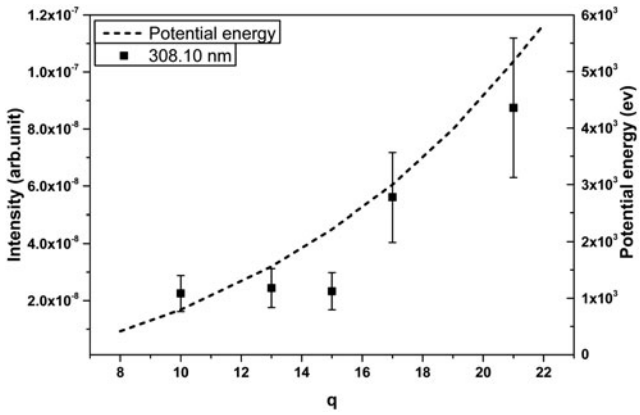

Fig. 8. Visible light intensity at 308.10 nm (A) and potential energy versus q.

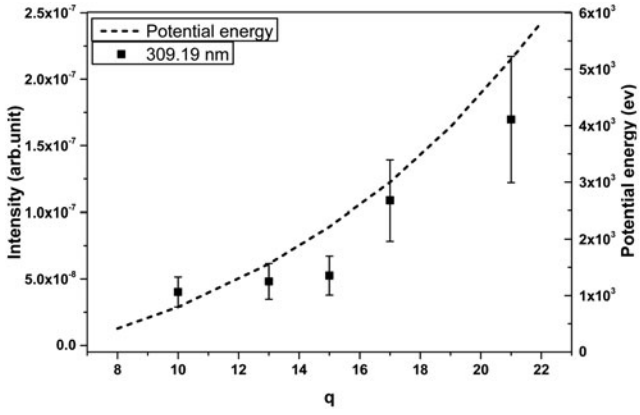

Fig. 9. Visible light intensity at 309.19 nm (B) and potential energy versus q.

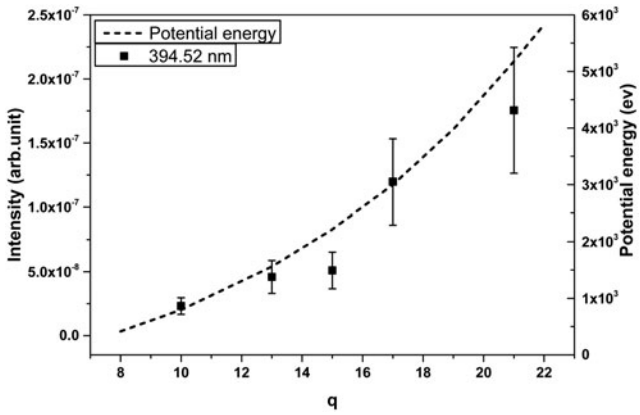

Fig. 10. Visible light intensity at 394.52 nm (C) and potential energy versus q.

(the total detected photon counts for each spectrum, obtained by integrating the peak using Gaussian fitting in OriginPro8) and the potential energy with the charge states are given in the following figures. The errors of the spectral intensity are slightly higher than 28%, including statistical and systematic errors. Specifically, the uncertainties from the electronics

https://doi.org/10.1017/S0263034616000628 Published online by Cambridge University Press

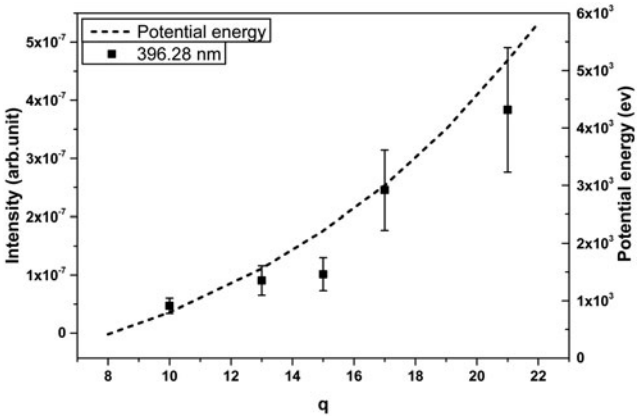

Fig. 11. Visible light intensity at 396.28 nm (D) and potential energy versus q.

noise are the main contribution to these errors, which contains the errors from the Spectra Hub (27%) and the refrigeration device (4%). Besides, the beam unstability brings an error about 5%. The spectral intensity versus the projectile charge state is shown on the left axis and the potential energy versus q is shown on the right axis in Figures 8–11.

As see from Figures 8–11, as the rise of q, the spectral intensity variation tendency is similar to that of the potential energy growth in the charge state range of 10–21. On the other hand, combining the solid state theory and the COB model, it gives a critical charge state 26, where the photon intensity will increase sharply with the higher q. Therefore, it tells us that, in the present experiment, the projectile neutralization process obeys the staircase COB model (Ducrée *et al.*, 1998). Unfortunately, it shows a large deviation between the experimental point and the potential curve when $q = 15$. The big deviation, origins from the experimental error, especially the beam instability.

4. CONCLUSIONS

In the present work, we have measured the visible light emission from the collisions of Xe^{q+} (q = 10–21) ions with the Al target at 410 keV. Spectrum wavelength in 300–500 nm is recorded. The visible light from the neutralization of the projectiles Xe II and the excited target Al I atoms are detected at the same time. It is shown that both Xe II and Al I photon intensities exhibit an incident charge state dependence, the larger q, the more visible light emission and they have a same variation tendency with the potential energy. It indicates that our results agree well with the staircase COB model.

ACKNOWLEDGMENT

This work is supported by National Natural Science Foundation of China (NSFC) (Grants Nos. 11174296). We would like to thank the staff of 320 kV platform for arrangement and operation of the ion source.

REFERENCES

Bajales, N., Cristina, L., Mendoza, S., Baragiola, R.A., Goldberg, E.C. & Ferrón, J. (2008). Exciton autoionization in ion-induced electron emission. *Phys. Rev. Lett*. **100**, 227604-1–4.

Burgdörfer, J., Lerner, P. & Meyer, F. (1991). Above-surface neutralization of highly charged ions: The classical-over-the-barrier model. *Phys. Rev. A* **44**, 5674–5685.

Dietrich, K.-G., Hoffmann, D.H.H., Wahl, H., Haas, C.R., Kunze, H., Brandenburg, W. & Noll, R. (1990). Energy loss of heavy ions in a dense hydrogen plasma. *Z. Phys. D – Atoms Molecules Clusters* **16**, 229–230.

Ducrée, J.J., Casali, F. & Thumm, U. (1998). Extended classical-over-barrier model for collisions of highly charged ions with conducting and insulating surfaces. *Phys. Rev. A* **57**, 338–350.

Eriksson, K.B.S. & Isberg, H.B.S. (1963). The spectrum of atomic aluminum, Al I. *Ark. Fys. (Stockholm)* **23**, 527–542.

Golubev, A., Turtikov, V., Fertman, A., Roudskoy, I., Sharkov, B., Geissel, M., Neuner, U., Roth, M., Tauschwitz, A., WAHL, H., Hoffmann, D.H.H., Funk, U., Süß, W. & Jacoby, J. (2001). Experimental investigation of the effective charge state of ions in beam-plasma interaction. *Nucl. Instr. Meth. Phys. Res., Sec. A* **464**, 247–252.

Hägg, L., Reinhold, C.O. & Burgdörfer, J. (1997). Above-surface neutralization of slow highly charged ions in front of ionic crystals. *Phys. Rev. A* **55**, 2097–2108.

Hoffmann, D.H.H., Blazevic, A., Korostiy, S., Ni, P., Pikuz, S.A., Rethfeld, B., Rosmej, O., Roth, M., Tahir, N.A., Udrea, S., Varentsov, D., Weyrich, K., Sharkov, B.Y. & Maron, Y. (2007). Inertial fusion energy issues of intense heavy ion and laser beams interacting with ionized matter studied at GSI-Darmstadt. *Nucl. Instr. Meth. Phys. Res., Sec. A* **577**, 8–13.

Hoffmann, D.H.H., Blazevic, A., Ni, P., Rosmej, O., Roth, M., Tahir, N.A., Tauschwitz, A., Udrea, S., Varentsov, D., Weyrich, K. & Maron, Y. (2005). Present and future perspectives for high energy density physics with intense heavy ion and laser beams. *Laser Part. Beams* **23**, 47–53.

Jadoual, L., El Boujlaidi, A., Ait El Fqih, M., Aamouche, A. & Kaddouri, A. (2014). Optical emission from ion-bombarded nickel and nickel oxide. *Spectrosc. Lett*. **47**, 363–366.

Kudo, M., Sakai, Y. & Ichinokawa, T. (2000). Dependencies of secondary electron yields on work function for metals by electron and ion bombardment. *Appl. Phys. Lett*. **76**, 3475–3477.

Lemell, C., Winter, H.P., Aumayr, F., Burgdörfer, J. & Meyer, F. (1996). Image acceleration of highly charged ions by metal surfaces. *Phys. Rev. A* **53**, 880–885.

Mei, C.X., Zhao, Y.T., Zhang, X.A., Ren, J.R., Zhou, X.M., Wagn, X., Lei, Y., Liang, C.H., Li, Y.Z. & Xiao, G.Q. (2012). X-ray emission induced by 1.2–3.6 MeV Kr^{13+} ions. *Laser Part. Beams* **30**, 665–670.

Niehaus, A. (1986). A classical model for multiple-electron capture in slow collisions of highly charged ions with atoms. *J. Phys. B: At. Mol. Phys*. **19**, 2925–2937.

Rajasekar, P., Scott, D. & Materer, N.F. (2006). Light emission from ion-bombarded Ge(100) surfaces under continuous germane and silane exposures. *Nucl. Instr. Meth. Phys. Res., Sec. B* **245**, 411–420.

Ren, J.R., Zhao, Y.T., Zhou, X.M., Wang, X., Lei, Y., Xu, G., Cheng, R., Wang, Y.Y., Liu, S.D., Sun, Y.B. & Xiao., G.Q. (2015). Charge-state dependence of inner-shell processes in

https://doi.org/10.1017/S0263034616000628 Published online by Cambridge University Press

collisions between highly charged Xe ions and solids at intermediate energies. *Phys. Rev. A* **92**, 062710-1–6.

Ryufuku, H., Sasaki, K. & Watanabe, T. (1980). Oscillatory behavior of charge transfer cross sections as a function of the charge of projectiles in low-energy collisions. *Phys. Rev. A* **21**, 745–750.

Sakurai, M., Sasaki, K., Miyamoto, T., Kato, D. & Sakaue, H.A. (2016). Potential effects in the interaction of highly charged ions with solid surfaces. *e-J. Surf. Sci. Nanotech*. **14**, 1–3.

Schenkel, T., Hamza, A.V., Barnes, A.V. & Schneider, D.H. (1999). Interaction of slow, very highly charged ions with surfaces. *Prog. Surf. Sci*. **61**, 23–84.

Sekioka, T., Terasawa, M., Mitamura, T., Stockli, M.P., Lehnert, U. & Cocke, C.L. (1998). Electronic excitation effect in the sputtering of conductive materials bombarded by highly charged heavy ions. *Nucl. Instr. Meth. B* **146**, 172–177.

Song, Z.Y., Yang, Z.H., Zhang, H.Q., Shao, J.X., Cui, Y., Zhang, Y.P., Zhang, X.A., Zhao, Y.T., Chen, X.M. & Xiao, G.Q. (2015). Rydberg-to-M-shell x-ray emission of hollow Xe^{q+} ($q = 27$–30) atoms or ions above metallic surfaces. *Phys. Rev. A* **91**, 042707-1–7.

Sporn, M., Libiseller, G., Neidhart, T., Schmid, M., Aumayr, F., Winter, H.P. & Varga, P. (1997). Potential sputtering of clean sio_2 by slow highly charged ions. *Phys. Rev. Lett*. **79**, 945–948.

Sun, L.T., Li, J.Y., Zhang, X.Z., Wang, H., Ma, B.H., Li, X.X., Feng, Y.C., Song, M.T., Zhu, Y.H., Zhao, L.M., Wang, P.Z., Liu, H.P., Zhao, H.W., Ma, X.W. & Zhan, W.L. (2007). Commissioning test of LAPECR2 source on the 320 kV HV platform. *High Energy Phys. Nuclear Phys*. **31**(Suppl. I), 55–59.

Walmsley, I., Waxer, L. & Dorrer, C. (2001). The role of dispersion in ultrafast optics. *Rev. Sci. Instr*. **72**, 1–29.

Wang, J.J., Zhang, J., Gu, J.G., Luo, X.W. & Hu, B.T. (2009). Highly charged Arq+ ions interacting with metals. *Phys. Rev. A* **80**, 062902/1–9.

Winter, H. & Aumayr, F. (2002). Slow multicharged ions hitting a solid surface: From hollow atoms to novel applications. *Europhys. News* **33**, 215–217.

Xu, Z.F., Zeng, L.X., Zhao, Y.T., Wang, J.G., Wang, Y.Y., Zhang, X.A., Xiao, G.Q. & Li, F.L. (2012). Charge effect in secondary electron emission from silicon surface induced by slow neon ions. *Laser Part. Beams* **30**, 319–324.

Zeng, L.X., Xu, Z.F., Zhao, Y.T., Wang, Y.Y., Wang, J.G., Cheng, R., Zhang, X.A., Ren, J.R., Zhou, X.M., Wang, X., Lei, Y., Li, Y.F., Yu, Y., Liu, X.L., Xiao, G.Q. & Li, F.L. (2012). Contribution from recoiling atoms in secondary electron emission induced by slow highly charged ions from tungsten surface. *Laser Part. Beams* **30**, 707–711.

Zhang, X.A., Zhao, Y.T., Hoffmann, D.H.H., Yang, Z.H., Chen, X.M., Xu, Z.F., Li, F.L. & Xiao, G.Q. (2011). X-ray emission of Xe^{30+} ion beam impacting on Au target. *Laser Part. Beams* **29**, 265–268.

Zhao, Y.T., Hu, Z.H., Cheng, R., Wang, Y.Y., Peng, H.B., Golubev, A., Zhang, X.A., Lu, X., Zhang, D.C., Zhou, X.M., Wang, X., Xu, G., Ren, J.R., Li, Y.F., Lei, Y., Sun, Y.B., Zhao, J.T., Wang, T.S., Wang, Y.N. & Xiao, G.Q. (2012). Trends in heavy ion interaction with plasma. *Laser Part. Beams* **30**, 679–706.

Zhao, Y.T., Xiao, G.Q., Zhang, X.A., Yang, Z.H., Zhang, Y.P., Chen, X.M., Zhang, H.Q., Cui, Y., Shao, J.X., Xu, X. & Li, F.L. (2005). Threshold kinetic energy for gold x-ray emission induced by highly charged ions. *Int. J. Mod. Phys. B* **19**, 2486–2490.

https://doi.org/10.1017/S0263034616000628 Published online by Cambridge University Press